THE JOURNAL OF PHYSICAL CHEMISTRY B

Article

pubs.acs.org/JPCB

Modulation of the Extent of Cooperative Structural Change During Protein Folding by Chemical Denaturant

Prashant N. Jethva and Jayant B. Udgaonkar*

National Centre for Biological Sciences, Tata Institute of Fundamental Research, Bengaluru 560065, India

Supporting Information

ABSTRACT: Protein folding and unfolding reactions invariably appear to be highly cooperative reactions, but the structural and sequence determinants of cooperativity are poorly understood. Importantly, it is not known whether cooperative structural change occurs throughout the protein, or whether some parts change cooperatively and other parts change noncooperatively. In the current study, hydrogen exchange mass spectrometry has been used to show that the mechanism of unfolding of the PI3K SH3 domain is similar in the absence and presence of 5 M urea. The data are well described by a four state N ↔ I_N ↔ I_2 ↔ U model, in which structural changes occur noncooperatively during the N ↔ I_N and I_N ↔ I_2 transitions, and occur cooperatively during the I_2 ↔ U transition. The nSrc-loop and RT-loop, as well as β strands 4 and 5 undergo noncooperative unfolding, while β strands 1, 2, and 3 unfold cooperatively in the absence of urea. However, in the presence of 5 M urea, the unfolding of β strand 4 switches to become cooperative, leading to an increase in the extent of cooperative structural change. The current study highlights the relationship between protein stability and cooperativity, by showing how the extent of cooperativity can be varied, using chemical denaturant to alter protein stability.

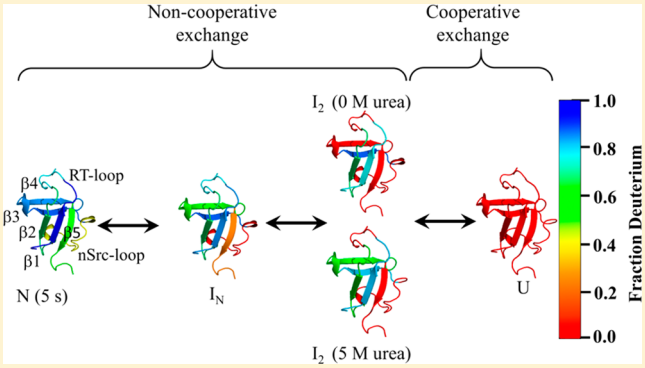

INTRODUCTION

Proteins possess dynamic structures.[1] A folded protein remains in equilibrium with many partially unfolded to completely unfolded states that are higher in free energy than the native (N) state.[2−6] The identification and characterization of such partially unfolded intermediate states on the free energy landscape, as well as of the cooperativity of the transitions to these states, remain a central goal of protein folding studies.[7−9] The sampling of these intermediates can be facilitated by suitable manipulation of pH, temperature, pressure, or chemical denaturants, such as urea and guanidine hydrochloride (GdnHCl). Despite chemical denaturants being used for many years to unfold proteins, little is known about how they affect the intrinsic dynamics of folded proteins,[10] and how they thereby affect the cooperativity of protein unfolding reactions.[11]

A denaturant may act by interacting directly with a protein, or by perturbing water structure, or by doing both. It appears that urea drives protein unfolding by directly and preferentially interacting with the polypeptide backbone.[12−16] Direct interaction of urea with the polypeptide backbone is not surprising, because of the similarity in their chemical structures; the carbonyl oxygen of urea can hydrogen bond to the amide hydrogen of the polypeptide backbone.[15,17] But how such interactions modulate the dynamical coupling of conformational change within and between secondary structural units, which are specified by backbone hydrogen bonding, is not clear. It is therefore important to compare and understand the intrinsic dynamics of a protein in the presence and absence of a denaturant.

Proteins sample high free energy intermediate states via a range of structural openings.[6,18−21] Such intermediates can be studied using techniques, such as native state thiol labeling,[2,22−24] nuclear magnetic resonance (NMR),[25,26] and by hydrogen exchange (HX) techniques.[18,27] HX coupled to mass spectrometry (HX-MS) provides information about the temporal evolution of coexisting populations of different structural forms of the protein, and can resolve between noncooperative and cooperative unfolding.[11,27−31] Hence, in the current study, HX-MS has been used to characterize the native-state dynamics of the PI3K SH3 domain in the presence and absence of urea, to understand the cooperativity of the conformational transitions that the protein can undergo.

The PI3K SH3 domain is an 82 residues-long protein, in which five β strands and one helix-like loop are arranged in a closed β barrel-like fold.[32] While it was originally thought to be a "two-state" folder,[33,34] studies utilizing multiple spectroscopic probes have revealed intermediate states.[35−37] The PI3K SH3 domain undergoes a nonspecific collapse early during folding,[38] and transient non-native tryptophan (Trp) burial early during

Received: May 10, 2017
Revised: August 2, 2017
Published: August 3, 2017

DOI: 10.1021/acs.jpcb.7b04473
J. Phys. Chem. B 2017, 121, 8263−8275

the unfolding.[39] The equilibrium unfolding curves of the PI3K SH3 domain carried out using either urea or GdnHCl showed significant slopes in the pre and post unfolding transition baselines,[35] suggesting that the native and unfolded state ensembles are sensitive to solvent conditions.[40−43] A previous native-state dynamics study of the PI3K SH3 domain by HX-MS in the absence and presence of GdnHCl indicated that a native-like intermediate (I_N) is populated in both the solvent conditions.[44] The current study aims to understand how urea affects the cooperativity of partial unfolding and folding transitions of the PI3K SH3 domain.

The current study shows that the PI3K SH3 domain undergoes two kinds of structural opening events, non-cooperative and cooperative. Two partially unfolded intermediate states, I_N and I_2, are populated both in the presence and in the absence of urea. I_2 forms via noncooperative structural opening events, but the logarithm of the apparent rate constant of formation of I_2 shows a strong dependence on urea concentration, similar to that seen for the logarithm of the apparent rate constant of formation of the unfolded state (U), suggesting that I_2 is a high free energy intermediate state. The presence of urea leads to an increase in the cooperativity of the unfolding. In the absence of any denaturant, β strands 1, 2, and 3 unfold cooperatively, while the rest of the protein undergoes noncooperative unfolding. In the presence of 5 M urea, the structural opening of β strand 4 changes from being noncooperative to being cooperative; consequently, there is an overall increase in unfolding cooperativity.

EXPERIMENTAL METHODS

Protein Purification. The PI3K SH3 domain was purified as described previously.[35] The purity of the protein was assessed by electrospray ionization mass spectrometry (ESI-MS), which showed the expected mass of the protein of 9276 Da, and that the protein was >95% pure. The concentration of the purified protein was determined by measuring the absorbance at 280 nm, using an extinction coefficient of 17900 cm^{-1} M^{-1}.[45]

Chemicals and Buffers. All the reagents and buffers used were of the highest purity grade available from Sigma, unless otherwise specified. Urea was obtained from United States Biochemicals. Sodium phosphate (20mM), 20 mM 3-morpholinopropanesulfonic acid (MOPS), and 20 mM Tris HCl were used as buffers at pH 7.2, pH 6.2, and pH 8.2, respectively. To quench the exchange reaction, ice-cold 100 mM glycine hydrochloride, at pH 2.3, was added to obtain a final pH of 2.6. For exchange out in the presence of urea, the concentration of the urea was determined by refractive index measurements on an Abbe refractometer. The pH values reported were not corrected for the isotope effect.

Fluorescence Monitored Unfolding Kinetics. Urea-induced unfolding of the PI3K SH3 domain was monitored as described previously,[35] using a stopped-flow module (SFM4) from Biologic. An excitation wavelength of 268 ± 1 nm was used, and the fluorescence emission was collected at 300 ± 10 nm using a band-pass filter from Asahi Spectra. The final protein concentration used was 20 μM.

Deuteration of PI3K SH3 Domain. Protein was deuterated as described previously.[44] Briefly, the lyophilized protein was dissolved in 20 mM sodium phosphate buffer, pH 7.2, prepared in D_2O (protein concentration 500 μM). The solubilized protein was incubated at 70 °C for 10 min. After 10 min, the protein solution was immediately transferred on to ice for 30 min, after which it was equilibrated at 25 °C. For deuteration of the protein at pH 6.2 and 8.2, the same procedure was followed except 20 mM MOPS, pH 6.2 (prepared in D_2O) and 20 mM Tris HCl, pH 8.2 (prepared in D_2O) were used, respectively.

Hydrogen Exchange. To initiate the hydrogen exchange (HX) reaction, 5 μL of deuterated protein (500 μM, 20 mM sodium phosphate pH 7.2, D_2O) were diluted to 100 μL (20-fold dilution) with exchange buffer (with or without urea, 20 mM sodium phosphate pH 7.2, H_2O). For the HX reaction at pH 6.2 and 8.2, the same procedure was followed except that the deuterated protein at pH 6.2 and 8.2, and labeling buffer at pH 6.2 (20 mM MOPS prepared in H_2O) and at pH 8.2 (20 mM Tris HCl prepared in H_2O) were used, respectively. All the exchange reactions were carried out at 25 °C. At the specified time of exchange, the reaction was quenched by adding ice-cold 100 μL of 100 mM glycine-HCl, pH 2.3 in H_2O (resulting in an additional 2-fold dilution). For the back-exchange control (BKEX), the same labeling procedure was followed, except that deuterated labeling buffer was used (20 mM sodium phosphate, pH 7.2, D_2O) instead of protonated labeling buffer.

Sample Processing for ESI-MS. After quenching, the protein was desalted using a Sephadex G-25 Hi-trap desalting column attached to an ÄKTA basic HPLC system (GE Healthcare Life Sciences). Protein was eluted from the desalting column with ice-cold acidic water (pH was adjusted to 2.6 by formic acid). 50 μL of the desalted protein were injected into the HDX module attached to a nanoAcquity UPLC, which was coupled to a Synapt G2 HD mass spectrometer (Waters Corporation). In the HDX module, protein was first allowed to accumulate in a trap column (C18 reverse phase), followed by elution with a gradient of 3−40% acetonitrile in 2 min, at a flow rate of 40 μL/min. The eluted protein was infused online into the mass spectrometer. The entire chromatographic setup was maintained at 4 °C to minimize back-exchange in the HDX module.

Peptide Mapping. For peptide mapping, the desalted protein was injected into an immobilized pepsin column (Applied Biosystems), which was equilibrated with water containing 0.05% formic acid. Protein was passed through the pepsin column for a total of 4 min at a flow rate of 50 μL/min. The peptides thus generated were trapped using the trap column, and then separated using an analytical column (C18 reverse phase), with a gradient of 10−37% acetonitrile containing 0.1% formic acid in 10 min. To identify the peptides as well as their retention times, the MS/tandem MS^E method was used, followed by analysis using the ProteinLynx Global Server (PLGS, v2.4, from Waters Corporation).

Data Acquisition by ESI-MS. For acquiring MS data, the capillary voltage, source temperature, and desolvation temperature were kept at 3 kV, 35 °C, and 100 °C, respectively. To minimize carryover, 2 or 3 blank runs were carried out in between two sample runs.

Data Analysis. *Intact Protein.* The first 20 scans from the time the protein started eluting were combined. The spectra were further analyzed with the MassLynx software using the background subtraction, smoothen, and centroid functions. The signal was normalized with respect to the total area under the curve of the +11 charge state. The number of deuteriums (amide sites) retained (protected) was obtained by subtracting the centroid mass of protonated protein from the observed centroid mass of each exchanged sample. A plot of the number of deuteriums retained versus time of HX was fitted to either a

DOI: 10.1021/acs.jpcb.7b04473
J. Phys. Chem. B 2017, 121, 8263−8275

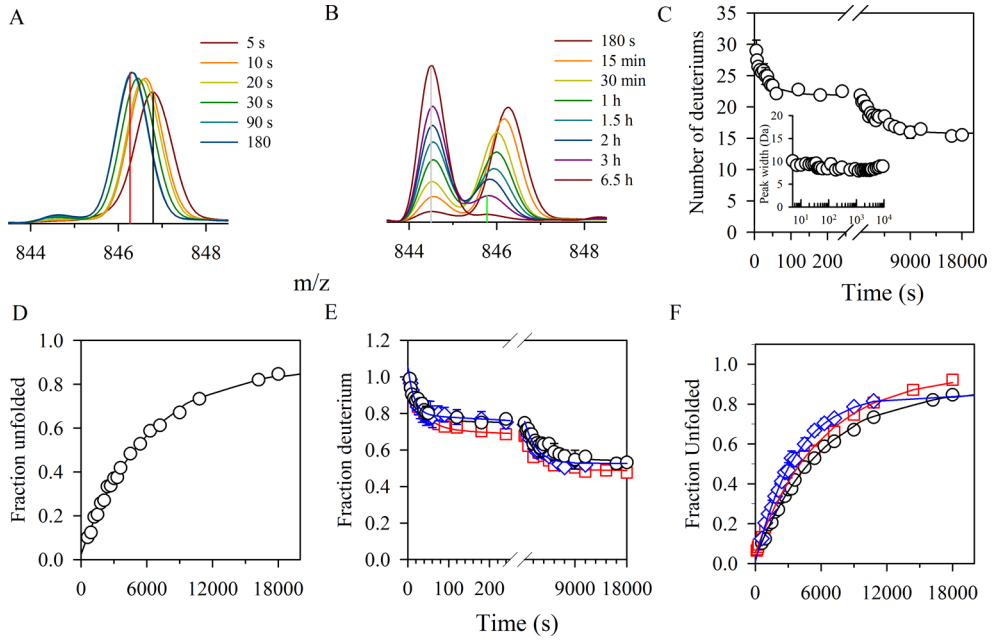

Figure 1. Kinetics of HX into the PI3K SH3 domain in the absence of urea at pH 7.2, 25 °C. Representative mass distributions (+11 charge state) are shown for exchange in the first 180 s (A) and from 180 s to 6.5 h (B). The solid vertical lines represent the centroid m/z values for the N state (5 s), U state (6.5 h), and for the partially unfolded intermediate states populated at the ends of the fast (red vertical line) and slow (green vertical line) kinetic phases of HX (panel C). (C) A plot of the number of deuteriums retained as a function of time of exchange was fitted to a double exponential equation (solid line). 30 ± 1 deuteriums are retained at 5 s of HX in the N state. The first 7 ± 1 deuteriums exchange out at a mean apparent rate constant of 3.5 ± 0.2 × 10^{-2} s^{-1}, and the next 7 ± 1 exchange out at a mean apparent rate constant of 3.0 ± 0.3 × 10^{-4} s^{-1}. The inset shows the dependence of the width at 50% of the peak height of the higher mass distribution on time of exchange. (D) The increase in the fraction of completely exchanged protein was fit to a single exponential equation (solid line), to yield a mean apparent rate constant of 1.4 ± 0.2 × 10^{-4} s^{-1}. (E) The fractional deuterium retention at pH 6.2 (red open square), pH 7.2 (black open circle), and pH 8.2 (blue open diamond) in the native-like forms (high mass distributions) is plotted versus time of exchange (data were normalized to the total amplitude of the HX reaction at 5 s, to account for the fact that more deuteriums were retained at lower pH, see Table S1, and were individually fit (solid lines) to determine the mean apparent rate constants for the fast noncooperative and slow noncooperative phases of HX at pH 6.2, 7.2, and 8.2, which are listed in Table S1. (F) The fraction of completely exchanged protein is plotted versus time of exchange at pH 6.2 (red open square), pH 7.2 (black open circle), and pH 8.2 (blue open diamond) were individually fit (solid lines) to determine the apparent rate constants of the cooperative phase at pH 6.2, 7.2, and 8.2, which are listed in Table S1. At the end of the HX reaction, the protein was found to retain 2 ± 1 deuteriums at pH 7.2, 25 °C, which was expected since HX was carried out in buffer containing 95% H_2O and 5% D_2O. The error bars in panels C, D, E, and F represent the spread in the data from two separate experiments and are smaller than the size of the symbols for most data points.

single or a double exponential function using the SigmaPlot software (v12), to determine the apparent rate constants and amplitudes of the HX reaction. The fractional deuterium retention was calculated as follows.[46]

$$\text{Fraction } D = \frac{(m_{(t)} - m_{(5\%D)})}{(m_{(100\%D)} - m_{(5\%D)})}$$

Here $m_{(t)}$ is the observed centroid mass at time t of exchange. The centroid mass of the back-exchanged sample (pH 7.2, 25 °C) was considered as the 100% deuterated control, and the centroid mass at 6.5 h of exchange (pH 7.2, 25 °C) was considered as the 5% deuterated control.

Peptide Analysis. The retention times of the peptides were identified using the PLGS software. In order to determine the centroid mass, as well as the width of the isotopic mass distribution at 20% of the distribution height, intensity values for the isotopic mass distributions were exported to HX-Express2, an Excel-based macro program.[47,48] The isotopic mass distributions of the peptides were fitted to either a single binomial (to deconvolute a unimodal pattern of exchange), or a double binomial (to deconvolute a bimodal pattern of exchange) function. The fractional deuterium content was calculated as for the intact protein. The plot of the fraction deuterium retained versus time was fitted to either a single or a double exponential equation to determine the apparent rate constants and amplitudes of the HX reaction.

Kinetic Simulation. The mass distribution of the +11 charge state at different times of HX in the absence of denaturant was globally fit to a kinetic mechanism in MATLAB (vR2011a). The function *fminsearchbnd* was used to determine the parameters of the kinetic mechanism. Details of the formulation of the kinetic mechanism are given in the Supporting Information.

RESULTS

HX in the Absence of Denaturant. The HX reaction was initiated by diluting the deuterated protein 20-fold into the protonated buffer at pH 7.2, 25 °C. The exchange was allowed to proceed for variable times before it was quenched by lowering the pH to 2.6. The back exchange control sample (BKEX) retained 44 ± 1 deuteriums. The mass distribution at 5 s of HX was unimodal (Figure 1A), and the centroid mass indicated that 30 ± 1 deuteriums were retained at this earliest time point of HX. Hence, out of 44 ± 1 amide sites, only 30 ± 1 were sufficiently protected to serve as structural probes at pH 7.2, 25 °C; the other amide sites (14 ± 1, ~ 30% D) exchanged out too rapidly to be monitored. Figure 1A,B shows how the

DOI: 10.1021/acs.jpcb.7b04473
J. Phys. Chem. B 2017, 121, 8263−8275

mass distribution evolved with time of exchange. For the first 180 s of HX, the mass distribution remained largely unimodal, but shifted gradually to lower mass. After 180 s of HX, the mass distribution became bimodal, with the appearance of a mass distribution corresponding to completely exchanged protein. Figure 1C shows that the centroid of the higher mass distribution shifted to lower mass in two kinetic phases, without any change in the width of the mass distribution (Figure 1C inset). Figure 1D shows that the relative amount of the completely exchanged protein increased exponentially with time, at a rate that was similar to the slower of the two kinetic phases of movement of the higher mass distribution (Table S1).

The N state that afforded protection to 30 ± 1 deuteriums, gradually lost 7 ± 1 deuteriums in the fast phase of noncooperative HX. The pause in HX before the slow phase of noncooperative HX suggested that a partially unfolded intermediate, I_N, was sampled transiently. During the slow phase of noncooperative HX, two processes appeared to occur simultaneously. In one process, some of the protein molecules giving rise to the high mass distribution, in which structure (I_N) afforded protection to 23 ± 1 deuteriums, lost a further 7 ± 1 deuteriums noncooperatively, leading to the transient formation of another partially unfolded intermediate, I_2. Simultaneously, all protein molecules, whether N, I_N, or I_2, appeared to lose their entire protective structure in a cooperative manner, leading to the transient formation of the completely unfolded (exchanged) protein (U).

It was important to determine whether the HX occurred in the EX1 or in the EX2 regime. The EX2 regime is observed when the apparent intrinsic rate constant of exchange, k_{int} is rate-limiting in the overall process of exchange, and it manifests itself in an HX-MS experiment as a single unimodal mass distribution which changes its centroid m/z position gradually with time of exchange. HX occurs in the EX1 regime when the apparent rate constant of structural opening to exchange is rate-limiting. In this case, HX-MS will usually, but not always[11,28,49,50] show a bimodal mass distribution whose individual peaks change in relative areas but not in position with time of exchange. In a previous study,[44] only 19 deuteriums were found to be protected in the protein at 5 s of exchange, and exchange was shown to occur in the EX1 regime. In the current study, it was observed that by taking care to minimize back-exchange of deuteriums,[51,52] the number of deuteriums retained by the protein at 5 s of exchange increased to 30 ± 1. In this context, it was important to determine whether HX still occurred in the EX1 regime, or whether the additional deuteriums probed, exchanged in the EX2 regime. The apparent rate constants of folding (0.3 s^{-1}) and unfolding (9×10^{-5} s^{-1}) of the PI3K SH3 domain[33,35] are much slower than the apparent intrinsic exchange rate constant of the PI3K SH3 domain at pH 7.2, 25 °C (25 s^{-1});[53] thus, the protein is expected to undergo HX in the EX1 regime. Figure 1E,F and Table S1 show that the apparent rate constants of all the observed kinetic phases of HX were similar at pH 6.2, 7.2, and 8.2. Since the observed apparent rate constants of HX in the EX2 regime would have changed 10-fold with a change in pH by 1 unit, it was clear that HX did occur in the EX1 regime (see also Supporting Information), in agreement with the earlier study.[44] It should be noted that both the stability and the global unfolding kinetics of the protein are the same at pH 6.2 and pH 7.2 (Figure S1) and pH 8.2, 25 °C.[44]

HX in the Presence of 5 M Urea. In 5 M urea, the PI3K SH3 domain is ~95% unfolded at equilibrium (C_m for the PI3K SH3 domain is 3.7 M urea).[35] The difference between unfolding in the absence and in the presence of a high concentration of denaturant, such as 5 M urea, is that the partially unfolded intermediates that are only very transiently sampled in the former case are likely to be stabilized and populated in the latter case. Moreover, all the unfolding transitions that involve an increase in the denaturant-accessible surface area are expected to occur at a faster rate. When HX was initiated simultaneously with unfolding in 5 M urea, pH 7.2, 25 °C, the changes in the mass distribution with time of HX were found to be qualitatively similar to those seen for HX in the absence of denaturant (Figure 2). The only difference was that all kinetic phases were faster. While the fast noncooperative phase leading to the formation of I_N was only 3-fold faster (Figure 2C), the slow noncooperative and cooperative phases leading to the formation of I_2 and U, respectively, were about 50-fold faster (Figure 2C,D). Another important observation was that as the urea concentration was

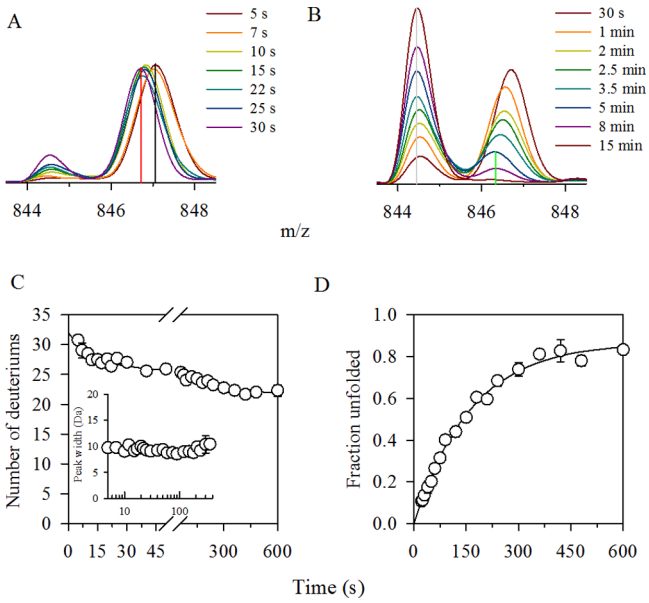

Figure 2. Kinetics of HX into the PI3K SH3 domain in the presence of 5 M urea at pH 7.2, 25 °C. Unfolding and HX were allowed to proceed simultaneously in 5 M urea for different times. At the end of the reactions (15 min), 95% of the protein molecules were found to be completely exchanged. Representative mass distributions (+11 charge state) are shown for exchange in the first 30 s (A) and from 30 s to 15 min (B). The solid vertical lines represent the centroid m/z values for the N state (5 s), U state (15 min), and for the partially unfolded intermediate states populated at the ends of the fast (red vertical line) and slow (green vertical line) kinetic phases of HX (panel C). (C) A plot of the number of deuteriums retained as a function of time of exchange was fitted to a double exponential equation (solid line). The first 5 ± 1 deuteriums exchange out at a mean apparent rate constant of 8.7 ± 0.6 × 10^{-2} s^{-1}, and the next 5 ± 1 exchange out at a mean apparent rate constant of 5.1 ± 0.6 × 10^{-3} s^{-1}. The inset shows the dependence of the width, at 50% of the peak height, of the higher mass distribution on time of exchange. (D) The increase in the fraction of completely exchanged protein was fitted to a single exponential equation (solid line), to yield a mean apparent rate constant of 6.5 ± 0.9 × 10^{-3} s^{-1}. At the end of the HX reaction, the protein was found to retain 2 ± 1 deuteriums at pH 7.2, 25 °C, which was expected since HX was carried out in buffer containing 95% H_2O and 5% D_2O. The error bars in panels C and D represent the spread in the data from two separate experiments.

DOI: 10.1021/acs.jpcb.7b04473
J. Phys. Chem. B 2017, 121, 8263−8275

increased from 0 to 5 M, the number of deuteriums that exchanged cooperatively progressively increased from 16 ± 1 in 0 M, to 22 ± 1 in 5 M urea (Table S1).

Urea Dependence of Opening/Unfolding Rate Constants. In the current study, two subdenaturing concentrations (1 and 3 M) apart from one denaturing concentration (5 M) of urea were used to determine the urea dependences for all the three kinetic phases (Figures S2 and S3). Figure 3 shows that

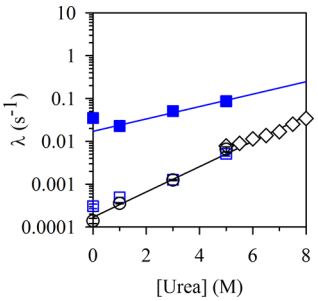

Figure 3. Urea dependence of the apparent rate constants of the different kinetic phases of HX into the PI3K SH3 domain at pH 7.2, 25 °C. (black open diamond), apparent global unfolding rate constants monitored by the intrinsic Tyr fluorescence measurement; (black open circle), apparent rate constants of appearance of completely exchanged protein; (blue closed square) and (blue open square), apparent rate constants of formation of I_N and I_2, respectively. The apparent rate constants of formation of I_N and I_2 were determined from the shift in the centroid of mass distribution of the native-like forms (high mass distribution) with time. The blue solid line is a linear fit (slope $m^{\ddagger}$ = 0.09 M^{-1}) to the dependence of the logarithm of the apparent rate constants of formation of I_N on urea concentration. The black solid line is a linear fit (slope $m^{\ddagger}$ = 0.28 M^{-1}) to the combined dependence on urea concentration of the logarithm of the apparent rate constants of global unfolding monitored by measurement of Tyr fluorescence change as well as by HX measurements. For the dependence of the logarithm of the apparent rate constants of global unfolding, the slope $m^{\ddagger}$ = 0.29 M^{-1}, and for that of slow noncooperative HX, the slope $m^{\ddagger}$ = 0.25 M^{-1}. The error bars represent the spread in the data from two separate experiments.

the logarithm of the apparent rate constant for the formation of I_N has a weak dependence on urea concentration. Hence, either very little surface area becomes exposed in the transition state (TS) of unfolding of N to I_N, or urea cannot bind to this TS. The dependences of the apparent rate constants of formation of I_2 and U fell on the linear extrapolation of the dependence of the logarithm of the apparent global unfolding rate constants on high urea concentrations. The latter were measured by monitoring the change in the intrinsic Tyr fluorescence of the protein. The observation that at low concentration of urea, the apparent global unfolding rate constants monitored by HX were in good agreement with the apparent global unfolding rate constants monitored by intrinsic Tyr fluorescence indicates that both probes monitor the formation of the same unfolded state. The kinetic phases corresponding to the formation of I_2 and U not only had strong but also similar dependences on urea concentration.

Mechanism of Unfolding. It was important to elucidate the kinetic mechanism for HX under native-like conditions. The assumptions made to do this, the manner in which global fitting was carried out, as well as the constraints used in the fitting simulations, are described in the Supporting Information. A linear four-state mechanism (Figure S4A) was found to be the simplest mechanism that explains all the native state HX data (Figure S4B). This mechanism also suggests that the formation of I_2 from I_N is the rate-limiting step for the unfolding of the PI3K SH3 domain.

Structural Characterization of the Partially Unfolded Intermediates Observed in HX in the Absence of Denaturant. In order to obtain structural information on the different regions of the protein undergoing exchange, peptic fragmentation of the protein was carried out at low pH, after the HX reaction was quenched, and the different sequence segments were identified by mass spectrometry. The fragments corresponding to different sequence segments of the protein had been identified earlier (Figure S5). Each sequence segment was separated by chromatography, and the fraction deuterium retained (fraction amide sites protected) in each sequence segment, averaged over all the amide sites within the fragment, was then determined. In this manner, the fraction deuterium retained at different times of HX was determined for each sequence segment.

Figure 4 shows the isotopic mass distributions of different sequence segments at different times of HX in the absence of denaturant. The mass distributions of sequence segments 1−11 (β strand 1), 23−35 (β strand 2), and 51−71 (β strands 3 and 4) became bimodal at later times of HX, indicating cooperative structural opening. Moreover, among these three sequence segments, two sequence segments, 1−11 (β strand 1) and 51−71 (β strands 3 and 4), showed noncooperative exchange out too. The high mass distribution corresponding to sequence segment 23−35 (β strand 2) was not observed to undergo any noncooperative exchange with time of exchange. Sequence segments 12−22 (RT-loop), 36−50 (nSrc-loop), 59−71 (β strand 4), and 71−81 (β strand 5) showed only gradual shifts in their mass distributions with time of HX, indicating that HX occurred only via the noncooperative phase of exchange out, and not during the cooperative structural opening phase.

It is important to note that due to the large number of deuteriums that were observed to be protected in the current study, it was possible to get quantitative information (Figure 5, Table 1) for exchange out in each sequence segment, which was not possible in a previous study.[44] The intact protein lost protection at 14 ± 1 out of 44 ± 1 deuteriums within the first 5 s of HX, and hence, all the sequence segments showed the initial drop in deuterium content in the first 5 s of HX, albeit to different degrees (Figure 5H and Table 1). The apparent rate constants of HX into the individual sequence segments (Figure 5) can be compared to the apparent rate constants of HX into the intact protein (Table 1) and to the apparent rate constants describing the N ↔ I_N ↔ I_2 ↔ U mechanism (Figure S4). By doing so, it becomes possible to determine at which step of the four-state mechanism, does each sequence segment unfold. The observed apparent rate constants of noncooperative HX into sequence segments 36−50 (nSrc-loop) and 12−22 (RT-loop) suggest that they exchange during the N ↔ I_N and I_N ↔ I_2 transition, respectively. Noncooperative HX into sequence segments 59−71 (β strand 4) and 71−81 (β strand 5) occurred in two kinetic phases whose apparent rate constants suggest that these sequence segments unfold (open) both during the N ↔ I_N and the I_N ↔ I_2 transitions.

The bimodal mass distributions for sequence segments 1−11 (β strand 1), 23−35 (β strand 2), and 51−71 (β strands 3 and 4) were deconvoluted into high and low (completely exchanged sequence segment) mass distributions. Figure 5G shows that the fractional U population calculated at different times of exchange, from the isotopic mass distribution of completely

DOI: 10.1021/acs.jpcb.7b04473
J. Phys. Chem. B 2017, 121, 8263−8275

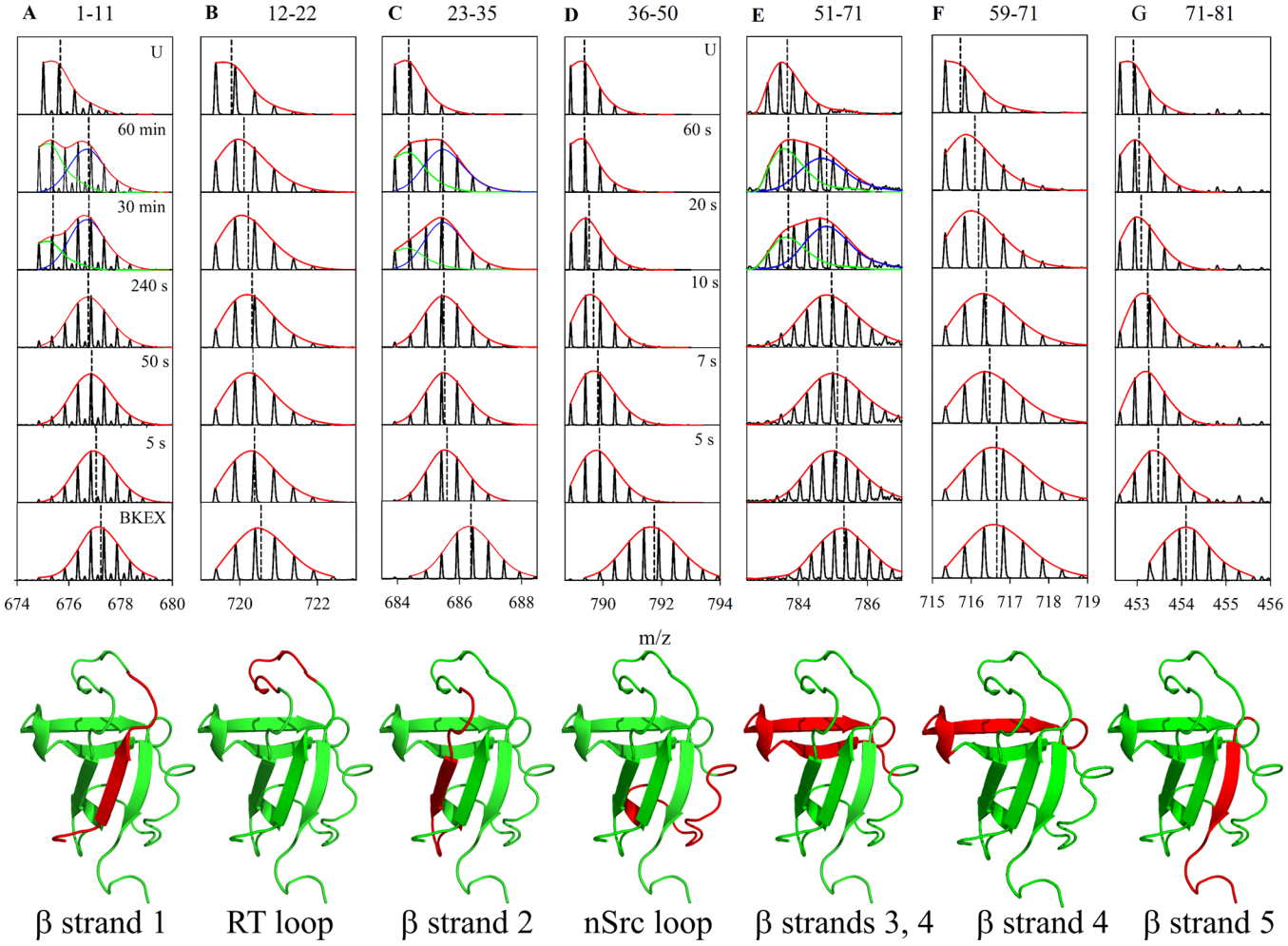

Figure 4. Isotopic mass distributions of representative peptide fragments obtained by proteolysis after different times of HX in the absence of denaturant at pH 7.2, 25 °C. The isotopic mass distributions of peptide fragments corresponding to sequence segments 1−11 (A), 12−22 (B), 23−35 (C), 36−50 (D), 51−71 (E), 59−71 (F), and 71−81 (G), are shown at the start of fast kinetic phase (5 s), at the middle of the fast kinetic phase of HX (50 s), at the end of the fast kinetic phase (240 s), and at 30 and 60 min, when cooperative exchange occurs. For sequence segment 36−50, which undergoes complete exchange within 60 s; data are shown for 5, 7, 10, 20, and 60 s. Also shown are the isotopic distributions of the BKEX and U (6.5 h) sequence segments. In each panel, the red line is the envelope of the observed isotopic mass distribution. The dashed vertical lines indicate the centroid m/z values of the unimodal distributions seen in panels B, D, F, and G and of the bimodal distributions seen in panels A, C, and E. The blue and green lines are the deconvoluted high mass and low mass distributions, respectively. Below each panel, the structure of the protein is shown, highlighting the relevant sequence segment. The structures are drawn using Pymol and PDB ID 1PNJ.

exchanged sequence segments (1−11, 23−35, and 51−71) agreed well with the appearance of U as measured for the intact protein in the absence of denaturant. Sequence segment 59−71 (β strand 4) did not show cooperative opening (Figure 4F), indicating, that only sequence segment 51−58 (β strand 3), a small part of the bigger segment 51−71 (β strands 3 and 4) exchanged cooperatively. Furthermore, quantification of the shift in the mass distribution with time of HX for both sequence segments (51−71 and 59−71) suggested that sequence segment 59−71 (β strand 4) was responsible for the shift in the high mass distribution observed for sequence segment 51−71, and hence, sequence segment 51−58 did not participate in noncooperative openings. HX into the sequence segment 1−11 also occurred during the fast and slow phases of noncooperative exchange (Figure 5A). The apparent rate constants of the fast and slow phases of noncooperative exchange were found to agree well the with apparent rate constants of formation of I_N and I_2, suggesting that sequence segment 1−11 also exchanged during the $N \leftrightarrow I_N$ and $I_N \leftrightarrow I_2$ transitions (Table 1).

The data in Figure 5H show that the 14 ± 1 deuteriums that lost protection within first 5 s of HX into the intact protein were lost from the nSrc-loop, RT-loop, and β strands 2 and 5. It should also be noted that while the intact protein had 30 ± 1 protected deuteriums after 5 s of HX, the peptic fragments together retained only a total of 16 ± 1 deuteriums. It is known[53] that the amide hydrogens belonging to the first two residues of a peptide fragment exchange too fast for their exchange to be observed. This is likely to be the reason why the count of the protected deuteriums in all the sequence segments is less than the count in the intact protein.

Structural Characterization of Partially Unfolded Intermediates Observed during Unfolding in the Presence of 5 M Urea. Figure S6 shows the mass distributions corresponding to different sequence segments at different time of HX in the presence of 5 M urea. Sequence segments 36−50 (nSrc-loop), 12−22 (RT-loop), and 71−81 (β

DOI: 10.1021/acs.jpcb.7b04473
J. Phys. Chem. B 2017, 121, 8263−8275

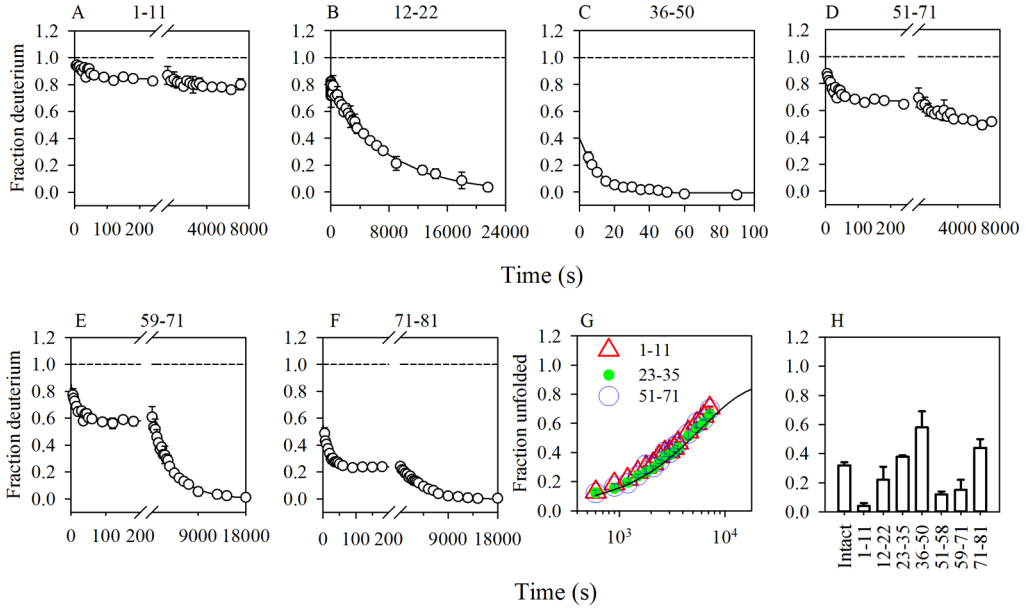

Figure 5. Kinetics of HX into different sequence segments in the absence of urea at pH 7.2, 25 °C. Panels A, B, C, D, E, and F shows the fraction deuterium retained versus time for the fast and slow phases of HX into sequence segments 1−11, 12−22, 36−50, 51−71, 59−71, and 71−81, respectively. The solid lines in the panels are either a single (panels B and C) or a double exponential (panels A, D, E, and F) fit to the data. The kinetic parameters describing the deuterium exchange out for each of the segments are listed in Table 1. The black dashed line indicates a value of 1 for the fraction deuterium retention in the BKEX sample. (G) The relative amounts of completely exchanged segments, which were obtained from deconvolution of the bimodal distribution (Figures 4A, C, and E), versus time of HX. The black solid line indicates the single exponential fit that was obtained from the plot of the fraction unfolded versus time for the intact protein in the absence of urea (Figure 1D). (H) Fractional decrease in deuterium during the first 5 s of HX. The error bars represent the spread in the data from two separate experiments.

strand 5) showed a continuous shift in the mass distribution with time of HX, indicating that they exchanged protected deuterium by the opening of one amide site at a time. As observed for HX in the absence of urea, the shift in the centroid of the mass distribution for sequence segments 36−50 and 12−22 fits to a single exponential equation, while for the sequence segment 71−81 the shift fit to a double exponential eq (Figure 6) The apparent rate constants obtained from the fits indicated that sequence segment 36−50 exchanged out during the formation of I_N, sequence segment 12−22 exchanged out during the formation of I_2, and that sequence segment 71−81 exchanged out during the formation of I_N as well as of I_2 (Table 1).

Sequence segments 1−11, 23−35, and 51−71 showed bimodal mass distributions with time of HX indicating cooperative opening as observed for HX in the absence of urea. Unlike in the absence of urea, sequence segment 59−71 showed bimodal mass distribution for HX in the presence of 5 M urea, indicating that it underwent cooperative opening in the presence of 5 M urea. Figure 6G shows that the fractional U population calculated as the fraction of segment that had completely exchanged at different times of exchange, from the isotopic mass distributions of sequence segments 1−11, 23−35, 51−71, and 59−71 agreed well with the appearance of U as measured for the intact protein in the presence of 5 M urea. This suggests that β strands 1, 2, 3, and 4 forms the cooperatively unfolding core of protein in the presence of 5 M urea, while only β strands 1, 2, and 3 form the cooperatively unfolding core in the absence of urea.

In the presence of 5 M urea, the centroids of the high mass distributions corresponding to the sequence segments 1−11 and 51−71 were found to be at higher m/z than seen in the absence of urea, indicating that the species which opened cooperatively contained more protected deuteriums. Figure 7 shows representative mass distributions of sequence segments 1−11 and 51−71 after HX in the absence and presence of 5 M urea. For both the sequence segments the width of the mass distribution was observed to be higher for HX in the presence of urea, indicating that the cooperativity was higher in the presence of 5 M urea. Sequence segment 1−11 was observed to exchange out 76% of its deuteriums cooperatively in the absence of urea, and 82% in the presence of 5 M urea (Table 1). In the case of sequence segment 51−71, the fraction of deuterium exchanging out cooperatively increased from 48% in 0 M urea to 70% in the presence of 5 M urea. Quantitative analysis showed that the reason behind the increase in the fraction of cooperatively exchanging deuterium was sequence segment 59−71. Sequence segment 59−71 exchanged its deuterium noncooperatively in two kinetic phases in the absence of denaturant (Figures 4F and 5E), and deuteriums that exchanged out during the second phase of noncooperative exchange in the absence of urea were found to exchange cooperatively in the presence of 5 M urea (Figures 6E and S6F) (see above). Hence, sequence segment 51−71 became more cooperative only because of sequence segment 59−71 becoming cooperative in the presence of 5 M urea. Sequence segment 51−58 appeared not to undergo any change in its HX behavior.

Sequence segments 1−11, 51−71, and 59−71 also exchanged noncooperatively, and the apparent rate constants for the shift in the mass distribution for all three agreed well with the apparent rate constant of formation of I_N. As observed for HX in the absence of urea, sequence segment 51−71 showed the fast phase of noncooperative exchange because of the smaller sequence segment 59−71. As in the absence of denaturant, sequence segment 23−35 (β strand 2) was not observed to

DOI: 10.1021/acs.jpcb.7b04473
J. Phys. Chem. B 2017, 121, 8263−8275

Table 1. Kinetics of the Fast and Slow Phases of HX, into Different Sequence Segments of the PI3K SH3 Domain at pH 7.2, 25 °C in the Absence and in the Presence of 5 M Urea[a]

sequence segment	Deuterium retention at 5 s	fast phase of noncooperative exchange		slow phase of noncooperative exchange		cooperative exchange	
		apparent rate constant x 10^{-2} (s^{-1})	deuterium exchange out	apparent rate constant x 10^{-4} (s^{-1})	deuterium exchange out	apparent rate constant x 10^{-4} (s^{-1})	deuterium exchange out
Intact Protein	**0.68 ± 0.05 (30.0 ± 1.0)**	3.5 ± 0.2	0.16 ± 0.02 (7.0 ± 1.0)	3.0 ± 0.3	0.16 ± 0.02 (7.0 ± 1.0)	1.4 ± 0.2	0.36 ± 0.02 (16.0 ± 1.0)
	0.72 ± 0.02 (32.0 ± 1.0)	8.7 ± 0.6	0.11± 0.02 (5.0 ± 1.0)	51.0 ± 6.0	0.11± 0.02 (5.0 ± 1.0)	65.0 ± 9.0	0.50± 0.02 (22 ± 1.0)
All segments	**0.71 ± 0.03 (15.5 ± 0.2)**	5.1 ± 0.4	0.21 ± 0.04 (4.5 ± 0.2)	2.3 ± 0.5	0.15 ± 0.03 (3.2 ± 0.1)	2.1 ± 0.6	0.36 ± 0.02 (7.8 ± 0.2)
	0.64 ± 0.07 (14.9 ± 0.1)	8.0 ± 3.0	0.13 ± 0.01 (3.0 ± 0.1)	72.0 ± 10.0	0.10 ± 0.01 (2.3 ± 0.1)	58.0 ± 20.0	0.41 ± 0.02 (9.7 ± 0.1)
36-50 (nSrc-loop)	**0.43 ± 0.13 (1.8 ± 0.3)**	9.3 ± 2.6	0.43 ± 0.13 (1.8 ± 0.3)				
	0.25 ± 0.10 (1.2 ± 0.5)	22.0 ± 6.0	0.25 ± 0.10 (1.2 ± 0.1)				
12-22 (RT-loop)	**0.78 ± 0.09 (1.0 ± 0.1)**			1.3 ± 0.1	0.80 ± 0.11 (1.0 ± 0.1)		
	0.78 ± 0.03 (1.3 ± 0.1)			72.0 ± 1.0	0.78 ± 0.03 (1.3 ± 0.1)		
71-81 (β strand 5)	**0.56 ± 0.06 (2.0 ± 0.2)**	6.5 ± 1.0	0.32 ± 0.06 (1.1 ± 0.2)	2.1 ± 0.1	0.25 ± 0.01 (0.9 ± 0.1)		
	0.45 ± 0.02 (1.6 ± 0.1)	9.1 ± 5.0	0.15 ± 0.02 (0.5 ± 0.1)	72.0 ± 20.0	0.29 ± 0.02 (1.0 ± 0.1)		
1-11 (β strand 1)	**0.96 ± 0.02 (3.5 ± 0.1)**	2.4 ± 0.6	0.11 ± 0.01 (0.4 ± 0.1)	3.5 ± 1.5	0.08 ± 0.01 (0.3 ± 0.1)	1.6 ± 0.1	0.76 ± 0.04 (2.8 ± 0.1)
	0.91 ± 0.01 (3.5 ± 0.1)	2.2 ± 1.0	0.09 ± 0.01 (0.4 ± 0.1)	Absent		70.0 ± 1.0	0.82 ± 0.02 (3.2 ± 0.1)
23-35 (β strand 2)	**0.63 ± 0.05 (2.4 ± 0.1)**					1.7 ± 0.1	0.63 ± 0.05 (2.4 ± 0.1)
	0.62 ± 0.02 (2.4 ± 0.1)					95.0 ± 30.0	0.62 ± 0.02 (2.4 ± 0.1)
51-71 (β strands 3 and 4)	**0.92 ± 0.06 (4.8 ± 0.3)**	4.7 ± 2.0	0.23 ± 0.02 (1.2 ± 0.1)	3.3 ± 0.6	0.19 ± 0.01 (1.0 ± 0.1)	3.3 ± 0.6	0.49 ± 0.02 (2.6 ± 0.2)
	0.84 ± 0.04 (4.9 ± 0.1)	1.7 ± 0.3	0.15 ± 0.01 (0.9 ± 0.1)	Absent		65.0 ± 10.0	0.70 ± 0.05 (4.1 ± 0.1)
59-71 (β strand 4)	**0.85 ± 0.07 (2.2 ± 0.1)**	7.5 ± 2.0	0.24 ± 0.03 (0.6 ± 0.1)	2.4 ± 0.1	0.61 ± 0.01 (1.6 ± 0.1)		
	0.80 ± 0.03 (2.2 ± 0.1)	4.6 ± 3.0	0.16 ± 0.01 (0.4 ± 0.1)	Absent		85.0 ± 30.0	0.64 ± 0.02 (1.7 ± 0.2)
51-58^ (β strand 3)	**0.96 ± 0.02 (2.6 ± 0.2)**					3.3 ± 0.6	0.88 ± 0.02 (2.4 ± 0.2)
	0.78 ± 0.04 (2.6 ± 0.1)					65.0 ± 10.0	0.73 ± 0.05 (2.4 ± 0.1)

[a]The numbers in the white and gray colored rows were obtained for HX in the absence and presence 5 M urea, respectively. Deuterium retention at 5 s was obtained by subtracting the number of deuteriums that were found to have exchanged out at 5 s from the back exchange control. The data in column 2 shows the fractional change in deuterium content that has not occurred at 5 s along with the number of deuteriums (in brackets) yet to exchange out. The data in columns 4, 6, and 8 show the fractional decrease in deuterium content, along with the number of deuteriums that exchange out (in brackets) in each kinetic phase. The data in the row labeled "all segments" sums the changes in deuterium content that occur in all the segments, as well as rate constants that have been averaged across all segments. ^Sequence segment is a part of the bigger sequence segment 51−71. To determine the exchange out kinetics of sequence segment 51−58, the contribution of sequence segment 59−71 was subtracted from the data of sequence segment 51−71.

undergo any noncooperative exchange even in the presence of 5 M urea.

The apparent rate constants for the three kinetic phases and their dependences on urea concentration were measured for the individual sequence segments (Table 1). Figure S7A shows that for the N to I_N transition, the apparent rate constants for the individual sequence segments were dispersed around the apparent rate constants observed for the intact protein. In contrast, Figures S7B and S7C show that for the $I_N \leftrightarrow I_2$, and $I_2 \leftrightarrow U$ transitions, the dependences on urea concentration of the apparent rate constants for the individual sequence segments matched the dependences of the apparent rate constants of the intact protein. Figure 8 shows a structural representation of fraction deuterium retained in N, I_N, I_2, and U for HX in the absence and presence of 5 M urea.

DISCUSSION

Noncooperative versus Cooperative Structural Openings in the Absence of Denaturant. The variety of structural openings that a protein undergoes in native conditions,[3,6,54] which might be local, or global,[55] are easily probed by HX measurements.[18,56] To understand the nature of structural opening, whether noncooperative or cooperative, it is important to determine whether exchange occurs in the EX1, EX2, or EXX regime, at pH 7.2, 25 °C.[11,27,28,50,57] This was especially important because unimodal mass distribution may result from HX via noncooperative openings in either regime, while bimodal distributions only result from HX via cooperative openings in the EX1 regime.

Several observations regarding HX into the intact protein suggested that it occurs in the EX1 regime (1) The exchange

DOI: 10.1021/acs.jpcb.7b04473
J. Phys. Chem. B 2017, 121, 8263−8275

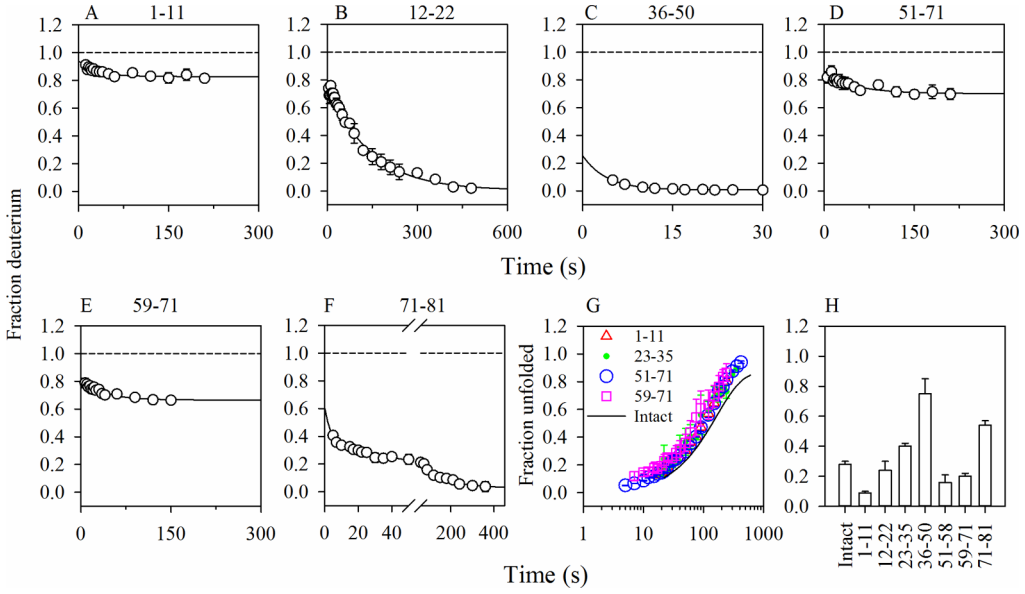

Figure 6. Kinetics of HX into different sequence segments in the presence of 5 M urea at pH 7.2, 25 °C. Panels A, B, C, D, E, and F shows the fraction deuterium retained versus time for the fast and slow phases of HX into sequence segments 1−11, 12−22, 36−50, 51−71, 59−71, and 71−81, respectively. The solid lines in the panels are either a single (panels A, B, C, D, and E) or a double exponential (panel F) fit to the data. The kinetic parameters describing the deuterium exchange out for each of the segments are listed in Table 1 (gray colored rows). The black dashed line indicates a value of 1 for the fraction deuterium retention in the BKEX sample. (G) The relative amounts of completely exchanged segments, which were obtained from deconvolution of the bimodal distribution (SI Figures S6 A, C, E, and F), versus time of HX. The black solid line indicates the single-exponential fit that was obtained from the plot of the fraction unfolded versus time for the intact protein in the presence of 5 M urea (Figure 2D). (H) Fractional decrease in deuterium during the first 5 s of HX. The error bars represent the spread in the data from two separate experiments.

rate constants of the two noncooperative phases as well as of the cooperative phase were the same at pH 6.2, 7.2 and 8.2, 25 °C (Figure 1E,F). (2) Bimodal mass distributions were observed at the later times of HX in the absence of denaturant, as well as in the presence of urea, which is conclusive proof that HX occurs in the EX1 regime. (3) The dependence on urea concentration of the apparent rate constant of the slow phases, both noncooperative and cooperative, of HX, extrapolated at zero denaturant to the values measured by HX in the absence of urea. (4) The width of the unimodal mass distributions seen during the fast and slow phases of noncooperative HX did not change with time of HX (Figures 1C and 2C). (5) For several sequence segments, the apparent rate constants for complete exchange were similar to the apparent rate constants for complete HX into the intact protein, both in the absence (Figure 5G) and presence of 5 M urea (Figure 6G).

The 30 ± 1 protected, and hence, slow exchanging amide hydrogens in the N state (Figure 1C) are expected to be hydrogen-bonded to the carbonyl groups of other residues.[58] The DSSP program[59] identified 33 hydrogen-bonded amide hydrogens in the protein. The intrinsic exchange rate constants (k_{int}) at pH 7.2, 25 °C were determined for these 33 amide hydrogens.[53] For each of these residues, the value of $\rho = \log k_{int}/k_{cl}$[60] was then determined using a value of 0.3 s^{-1} (see above) for k_{cl}, the rate constant for structure closing (see Supporting Information). It was found that 27 residues had $\rho \geq 1.3$, 2 had $\rho = 1.2$, 2 had $\rho = 1.1$, and 2 had $\rho = 1.0$. Thus, virtually all amide hydrogens had ρ values close to or greater than 1.3, which has been suggested to be the EX1 boundary.[60] Clearly, there is no correlation between the number of amide hydrogens that show noncooperative exchange (14) and the predicted ρ values of the structured amide sites.

In the fast phase of noncooperative exchange, during which the native state loses at 7 ± 1 deuteriums, the native state is in equilibrium with I_N. The members of the I_N ensemble differ very slightly from each other in their structural properties, in having just one or a few amide sites differently exposed.[61] Hence, a continuum of N-like states form during the N ↔ I_N transition, leading to a gradual shift in the centroid of the native-like high mass distribution. The kinetic pause observed before the start of the second phase of gradual, noncooperative exchange at another 7 ± 1 amide sites (Figure 1C), could be because critical tertiary interactions have to be broken before noncooperative transient exposure of amide sites continues during the transient formation of I_2. Hence, a continuum of partially unfolded intermediates is sampled during the transient formation of I_2 from I_N, which results in the gradual shift in the centroid of the high mass distribution in a manner similar to that observed during the formation of I_N. A kinetic pause is then observed, indicating that the transient sampling of conformations more unfolded than I_2, requires that critical interactions have first to be broken. These critical interactions appear to be extensive, because once they are broken; the protein samples the globally unfolded state. 16 ± 1 amide sites become exposed during the transient cooperative transition from I_2 to U.

Structural fluctuations observed in proteins are believed to be important for their function,[3,54] including in enzyme catalysis,[62] diffusion of ligand[63] and protein−protein interactions. It is possible that noncooperative openings could facilitate the binding of the PI3K SH3 domain to proline-rich sequences during signal transduction events. Although it has been suggested that native-state fluctuations in SH3 domains are important for their functions,[64] there is, at present, no experimental evidence which suggests that fluctuations of the PI3K SH3 domain are important for its function.

Structural Openings/Unfolding Modulated by the Presence of Urea. In three different urea concentrations,

DOI: 10.1021/acs.jpcb.7b04473
J. Phys. Chem. B 2017, 121, 8263−8275

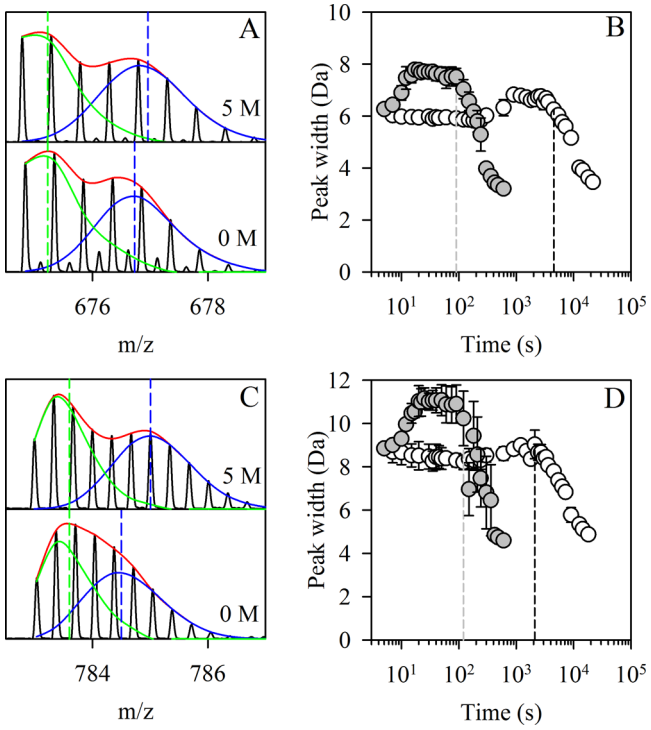

Figure 7. The increase in the cooperativity of the structural opening in the presence of 5 M urea at pH 7.2, 25 °C. Panels A and C shows the mass distributions for the sequence segments 1−11 and 51−71, respectively, at $t_{1/2}$ of global opening. Both the sequence segments exhibit a bimodal mass distribution suggesting cooperative opening. The red solid line is the observed isotopic mass distribution. The blue and green solid lines are the deconvoluted mass distributions for the high and low mass species, respectively. The vertical dashed lines indicate the centroid values for each mass distribution. The blue dashed lines for both the sequence segments are at higher m/z values in the presence of 5 M urea. Panels B and D show the kinetics of the change in the width of the mass distribution at 20% of the height of the isotopic mass distribution, for 5 M (gray filled circle) and 0 M (circle) urea, for the sequence segments 1−11 and 51−71, respectively. Both the sequence segments show an increase in peak width in the presence of 5 M urea. The vertical dashed lines in panels B and D correspond the $t_{1/2}$ values (90 s for 5 M urea and 75 min for 0 M urea), for both the sequence segments. Note that the time at which the peak width is maximum is difficult to determine directly because the maxima are broad. The error bars in panels B and D represent the spread in the data from two separate experiments.

ranging from native-like (1 M urea, Figure S2) to subdenaturing (3 M urea, Figure S3) to strongly denaturing (5 M urea, Figure 2), the PI3K SH3 domain was observed to exchange its protected deuteriums in three kinetic phases. The observation that the protein undergoes HX in two non-cooperative phases and a cooperative phase both in the absence and in the presence of urea, suggests that it samples the same conformational space it does in the absence as well as in the presence of urea.

The observation (Figure 3) that the dependence of the logarithm of the apparent rate constants for the formation of U, determined from the HX measurements, extrapolates linearly (within error) into the linear dependence seen for the logarithm of the apparent global unfolding measured by Tyr fluorescence, confirms that the cooperative phase of HX at all urea concentrations arises from global unfolding. This is an important observation especially since at zero and low urea

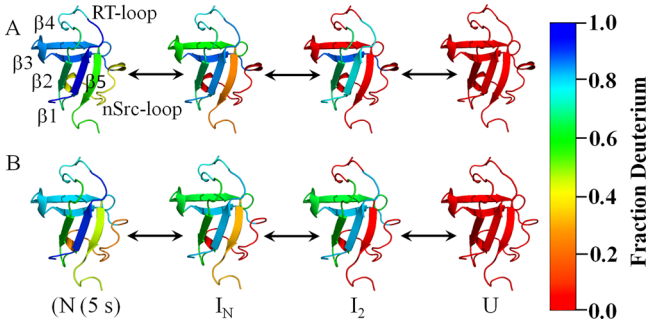

Figure 8. The structures of the partially unstructured intermediate states in the absence (A) and (B) in the presence of 5 M urea. The color bar indicates the fraction deuterium retained in the secondary structure elements in each state. For the N state, the fraction deuterium retained represents the deuterium that has not exchanged out at 5 s of HX. The structure of the PI3K SH3 domain is depicted using Pymol and the PDB file ID 1PNJ.

concentrations, the formation/sampling of U occurs very transiently, and it is only at 5 M urea that U is populated predominantly at equilibrium. The observation that the dependence on urea of the logarithm of the apparent rate constant for the formation of I_2 falls on that of the logarithm of the apparent rate constant for the formation of U was surprising. It suggests that both reactions are slowed down the same transition state. In other words, I_2 must form after the rate-limiting step of unfolding, like U (see Supporting Text). The observation that the linear dependence on urea concentration of the logarithm of the apparent rate constant for the formation of I_N is weak (Figure 3) suggests that the TS for the formation of I_N is very native-like.

The observation that the logarithm of the apparent rate constant of each kinetic phase, for both the intact protein (Figure 3) and for the individual sequence segments (Figure S7), has linear dependences on urea concentration indicates that urea facilitates the intrinsic dynamics of the protein by stabilizing the transition state preceding each intermediate state (Figure 3). Hence, it can be concluded that the mechanism of unfolding is not altered by the presence of urea, and that only the apparent rate constants are altered. The linear four-state mechanism (Figure S4) that describes transient unfolding in the absence of urea, therefore also describes complete (95%) unfolding in the presence of 5 M urea. The formation of I_2 from I_N is seen to be the rate-limiting step for the unfolding of the PI3K SH3 domain, from analysis according to this mechanism.

It should be noted that the closing rate constant (k_{cl}) in the presence of urea will be even slower than what it is in the absence of urea. Thus, the PI3K SH3 domain will undergo HX in the EX1 regime in the presence of urea too. It is because the PI3K SH3 domain exchanges in the EX1 regime that the time evolution of the mass distribution can be used to distinguish between noncooperative and cooperative openings, even though they have very similar apparent rate constants and denaturant dependences. Similar observations had been made previously for HX into the turkey ovomucoid third domain, which also occurred in the EX1 regime.[49]

Very recently, it has been shown that the cooperativity of folding/unfolding reactions can be manipulated by altering the stabilities of the N and U states.[11] That study predicted that when the U state is stabilized upon addition of urea, the unfolding of the PI3K SH3 domain should become more cooperative. This is precisely what is observed in the current

DOI: 10.1021/acs.jpcb.7b04473
J. Phys. Chem. B 2017, 121, 8263−8275

study. As the urea concentration was increased, the size of cooperative unit was found to increase from 16 ± 1 amide sites in the absence of urea, to 22 ± 1 amide sites in 5 M urea (Table S1). This urea concentration-dependent increase in the number of cooperatively opening amide sites had not been seen in the case of monellin,[11] wherein increasing GdnHCl increased the cooperativity of unfolding, but not the number of cooperatively opening amide sites. It appears that in the case of monellin, the size of cooperatively unfolding unit was maximum at the lowest GdnHCl concentration used.

Urea versus GdnHCl-Induced Unfolding. In a previous study of native-state HX of the PI3K SH3 domain in the presence of low concentrations of GdnHCl, unfolding was found to also proceed through the initial noncooperative formation of I_N.[44] In that study, however, while the transition from I_N to U was clearly not cooperative at low GdnHCl concentrations, the presence of I_2 could not be detected because the mass distribution of U was not sufficiently separated on the m/z scale from that of N. This was because exchange at fewer amide sites was studied because of technical limitations. Of course, it remains to be seen whether I_2 is actually populated during GdnHCl-induced unfolding. It should be noted that an unfolded-like intermediate, I_U has been shown to be populated during unfolding at high GdnHCl concentrations,[44] and it will be interesting to determine whether I_U is populated during unfolding at urea concentrations higher than 5 M. In the current study of urea-induced unfolding, the formation of I_N, I_2, and U each appear to occur via one pathway, as the logarithm of the apparent rate constant for the formation of each form does not have a nonlinear dependence on urea concentration (Figures 3 and S7).

Structural Changes under Native Conditions. The observations that the nSrc-loop and RT-loop exchanged out noncooperatively (Figure 4B and D), in single kinetic phases (Figure 5B,C), leading to the formation of I_N and I_2, respectively, suggested that both the loops behave as non-cooperatively opening units. Both loops had been found to be highly dynamic in a solution NMR study.[32] The RT-loop appears to have partial β strand character, and there is hydrogen bonding within the loop amides,[32] which might be responsible for the RT-loop not exchanging out during the initial formation of I_N, as does the nSrc-loop, but only later when I_N transforms into I_2. The observation that β strands 4 and 5 both exchange out in a noncooperative manner (Figure 4F,G), but that the centroids of the mass distributions of both the sequence segments shift in a double exponential manner (Figure 5E,F), suggests that both β stands have two groups of amide sites, one more protected than the other. The NMR structure suggests that both these β strands have a few amide sites that are solvent-exposed, and a few that are hydrogen bonded with other β strands (β strands 4 and 5 hydrogen bond with β strands 3 and 1, respectively). It is possible that amide sites which are not involved in hydrogen bonding exchange out during the transient formation of I_N, while amide sites which are involved in hydrogen bonding exchange slowly during the formation of I_2.

Sequence segments 1−11, 23−35, and 51−71 clearly show bimodal mass distributions, suggesting that β strands 1, 2, and 3 form the folded core of protein, which opens up cooperatively (Figures 5 and 6). β strand 1 also shows some noncooperative structural opening, indicating that some of the amide sites in this segment do not form part of the cooperatively unfolding unit. The RT-loop packs around β strands 3 and 4, while its ends are joined with β strand 1 and 2. Hence, any structural fluctuation which leads to the displacement of RT-loop is likely to lead to exposure of buried hydrophobic surface area and hence, led to global opening of the protein. Thus, when the RT-loop loses its structure during the formation of I_2, it leads to the cooperative opening of β strands 1, 2, and 3 during the subsequent formation of U (Figure 8A).

Figure 8A shows that in I_N, the nSrc-loop has exchanged out completely, while β strands 1, 4, and 5 have exchanged out partially. The rest of the structure in I_N remain native-like. In I_2, the RT-loop has additionally exchanged out completely, and β strands 4 and 5 have also completely lost their protective structure.

Structural Changes under Strongly Unfolding Conditions. From the mass distribution profiles (Figure S6) it is evident that the nSrc-loop, RT-loop, and β strand 5 undergo noncooperative structural openings in the presence of 5 M urea too. Figure 8B shows that the structure of I_N is the same in the presence of 5 M urea and in the absence of urea. The structure of I_2 is different in both the solvent conditions. Only the RT-loop and β strand 5 have exchanged out, while β strand 4 remains protected, during the formation of I_2 in 5 M urea. Thus, I_2 possesses more protective structure in 5 M urea than the absence of urea. The loss of structure in β strand 4 switching from being noncooperative in the absence of urea to being cooperative in the presence of 5 M urea, leading to an increase in the overall cooperativity of unfolding (Figure 7 and Table 1). Consequently, sequence segment 51−71 (β strands 4 and 5) shows a larger number of amide sites exchanging cooperatively in the presence of 5 M urea than in the absence of urea (Figure 7 and Table 1). The urea-induced increase in the cooperativity of unfolding could be due to the modulation of the stabilities of the ground states, and consequent movement of the transition state for unfolding from being unfolded-like in the absence of urea to being native-like in the presence of urea. The linear four state mechanism suggests that the TS of the $I_N \leftrightarrow I_2$ step is the rate-limiting TS for unfolding, and hence movement of the TS toward being more native-like could possibly lead to more protection in I_2, which unfolds cooperatively. β strand 1 too shows a slight increase in cooperativity, but the current peptide resolution is not sufficient to determine the amide site whose exchange becomes cooperative in the presence of 5 M urea.

■ CONCLUSION

The mechanism of unfolding of the PI3K SH3 domain is found to be the same in the absence of denaturant and in the presence of denaturant at high concentration. At high denaturant concentration, unfolding appears cooperative and two-state when monitored by ensemble-averaging probes. Nevertheless, HX-MS measurements in both the absence and presence of denaturant show that the cooperative structural change is restricted only to the buried, tightly packed core region of the protein. The rest of the protein undergoes structural change noncooperatively. Hence, the unfolding reaction is not two-state or all-or-none, as suggested by ensemble averaging probes. The barrier to the cooperative structural change occurring in a localized region of the protein dominates and conceals noncooperative structural change occurring elsewhere. The localized region undergoing cooperative structural change becomes larger when unfolding is carried out in the presence of chemical denaturant, indicating folding cooperativity is not

DOI: 10.1021/acs.jpcb.7b04473
J. Phys. Chem. B 2017, 121, 8263−8275

invariant, as generally thought, but can be modulated by solvent.

■ ASSOCIATED CONTENT

Supporting Information

The Supporting Information is available free of charge on the ACS Publications website at DOI: 10.1021/acs.jpcb.7b04473.

Theory of hydrogen exchange; mechanism of unfolding; fitting of linear four state mechanism of unfolding to HX data in the absence of urea; kinetics of the formation of U and the absence of a lag phase, HX, and fluorescence monitored unfolding at pH 6.2; unfolding dynamics in the presence of 1 and 3 M of urea; peptide intensity fits in the presence of 5 M urea; urea dependence of HX rate for all the peptide; and intact protein HX summary table (PDF)

■ AUTHOR INFORMATION

Corresponding Author

*E-mail: jayant@ncbs.res.in.

ORCID

Prashant N. Jethva: 0000-0002-7704-2810

Jayant B. Udgaonkar: 0000-0002-7005-224X

Notes

The authors declare no competing financial interest.

■ ACKNOWLEDGMENTS

We thank the members of our laboratory for discussions. J.B.U. is a recipient of a JC Bose National Research Fellowship from the Government of India. This work was funded by the Tata Institute of Fundamental Research, and by the Department of Science and Technology, Government of India.

■ ABBREVIATIONS

HX, hydrogen exchange; MS, mass spectrometry; TS, transition state; PI3K SH3 domain, SH3 domain of PI3 kinase; BKEX, back-exchange

■ REFERENCES

(1) Linderstrøm Lang, K. U.; Schellman, J. A. *Protein Structure and Enzyme Activity in "the Enzymes"*, 2nd ed.; Boyer, Lardy, Myrbäk, Eds.; Academic Press: New York, 1959; Vol. *1*, pp 443−510.

(2) Malhotra, P.; Udgaonkar, J. B. High-Energy Intermediates in Protein Unfolding Characterized by Thiol Labeling under Nativelike Conditions. *Biochemistry* **2014**, *53*, 3608−3620.

(3) Henzler-Wildman, K.; Kern, D. Dynamic Personalities of Proteins. *Nature* **2007**, *450*, 964−972.

(4) Epstein, D. M.; Benkovic, S. J.; Wright, P. E. Dynamics of the Dihydrofolate Reductase-Folate Complex: Catalytic Sites and Regions Known to Undergo Conformational Change Exhibit Diverse Dynamical Features. *Biochemistry* **1995**, *34*, 11037−11048.

(5) Frauenfelder, H.; Parak, F.; Young, R. D. Conformational Substates in Proteins. *Annu. Rev. Biophys. Biophys. Chem.* **1988**, *17*, 451−479.

(6) McCammon, J. A.; Gelin, B. R.; Karplus, M. Dynamics of Folded Proteins. *Nature* **1977**, *267*, 585−590.

(7) Bryngelson, J. D.; Onuchic, J. N.; Socci, N. D.; Wolynes, P. G. Funnels, Pathways, and the Energy Landscape of Protein Folding: A Synthesis. *Proteins: Struct., Funct., Genet.* **1995**, *21*, 167−195.

(8) Udgaonkar, J. B. Multiple Routes and Structural Heterogeneity in Protein Folding. *Annu. Rev. Biophys.* **2008**, *37*, 489−510.

(9) Malhotra, P.; Udgaonkar, J. B. How Cooperative Are Protein Folding and Unfolding Transitions? *Protein Sci.* **2016**, *25*, 1924−1941.

(10) Canchi, D. R.; García, A. E. Cosolvent Effects on Protein Stability. *Annu. Rev. Phys. Chem.* **2013**, *64*, 273−293.

(11) Malhotra, P.; Udgaonkar, J. B. Tuning Cooperativity on the Free Energy Landscape of Protein Folding. *Biochemistry* **2015**, *54*, 3431−3441.

(12) Auton, M.; Bolen, D. W. Predicting the Energetics of Osmolyte-Induced Protein Folding/Unfolding. *Proc. Natl. Acad. Sci. U. S. A.* **2005**, *102*, 15065−15068.

(13) Auton, M.; Holthauzen, L. M. F.; Bolen, D. W. Anatomy of Energetic Changes Accompanying Urea-Induced Protein Denaturation. *Proc. Natl. Acad. Sci. U. S. A.* **2007**, *104*, 15317−15322.

(14) Hua, L.; Zhou, R.; Thirumalai, D.; Berne, B. Urea Denaturation by Stronger Dispersion Interactions with Proteins Than Water Implies a 2-Stage Unfolding. *Proc. Natl. Acad. Sci. U. S. A.* **2008**, *105*, 16928−16933.

(15) Tirado-Rives, J.; Orozco, M.; Jorgensen, W. L. Molecular Dynamics Simulations of the Unfolding of Barnase in Water and 8 M Aqueous Urea. *Biochemistry* **1997**, *36*, 7313−7329.

(16) Lim, W. K.; Rösgen, J.; Englander, S. W. Urea, but Not Guanidinium, Destabilizes Proteins by Forming Hydrogen Bonds to the Peptide Group. *Proc. Natl. Acad. Sci. U. S. A.* **2009**, *106*, 2595−2600.

(17) O'Brien, E. P.; Dima, R. I.; Brooks, B.; Thirumalai, D. Interactions between Hydrophobic and Ionic Solutes in Aqueous Guanidinium Chloride and Urea Solutions: Lessons for Protein Denaturation Mechanism. *J. Am. Chem. Soc.* **2007**, *129*, 7346−7353.

(18) Bai, Y.; Sosnick, T. R.; Mayne, L.; Englander, S. W. Protein Folding Intermediates: Native-State Hydrogen Exchange. *Science* **1995**, *269*, 192−197.

(19) Bhuyan, A. K.; Udgaonkar, J. B. Stopped-Flow NMR Measurement of Hydrogen Exchange Rates in Reduced Horse Cytochrome C under Strongly Destabilizing Conditions. *Proteins: Struct., Funct., Genet.* **1998**, *32*, 241−247.

(20) Juneja, J.; Udgaonkar, J. B. Characterization of the Unfolding of Ribonuclease a by a Pulsed Hydrogen Exchange Study: Evidence for Competing Pathways for Unfolding. *Biochemistry* **2002**, *41*, 2641−2654.

(21) Chamberlain, A. K.; Handel, T. M.; Marqusee, S. Detection of Rare Partially Folded Molecules in Equilibrium with the Native Conformation of RNaseH. *Nat. Struct. Mol. Biol.* **1996**, *3*, 782−787.

(22) Sridevi, K.; Udgaonkar, J. B. Unfolding Rates of Barstar Determined in Native and Low Denaturant Conditions Indicate the Presence of Intermediates. *Biochemistry* **2002**, *41*, 1568−1578.

(23) Bernstein, R.; Schmidt, K. L.; Harbury, P. B.; Marqusee, S. Structural and Kinetic Mapping of Side-Chain Exposure onto the Protein Energy Landscape. *Proc. Natl. Acad. Sci. U. S. A.* **2011**, *108*, 10532−10537.

(24) Jha, S. K.; Dasgupta, A.; Malhotra, P.; Udgaonkar, J. B. Identification of Multiple Folding Pathways of Monellin Using Pulsed Thiol Labeling and Mass Spectrometry. *Biochemistry* **2011**, *50*, 3062−3074.

(25) Neudecker, P.; Robustelli, P.; Cavalli, A.; Walsh, P.; Lundström, P.; Zarrine-Afsar, A.; Sharpe, S.; Vendruscolo, M.; Kay, L. E. Structure of an Intermediate State in Protein Folding and Aggregation. *Science* **2012**, *336*, 362−366.

(26) Korzhnev, D. M.; Salvatella, X.; Vendruscolo, M.; Di Nardo, A. A.; Davidson, A. R.; Dobson, C. M.; Kay, L. E. Low-Populated Folding Intermediates of Fyn SH3 Characterized by Relaxation Dispersion NMR. *Nature* **2004**, *430*, 586−590.

(27) Miranker, A.; Robinson, C. V.; Radford, S. E.; Aplin, R. T.; Dobson, C. M. Detection of Transient Protein Folding Populations by Mass Spectrometry. *Science* **1993**, *262*, 896−900.

(28) Ferraro, D. M.; Lazo, N. D.; Robertson, A. D. EX1 Hydrogen Exchange and Protein Folding. *Biochemistry* **2004**, *43*, 587−594.

(29) Lanman, J.; Lam, T. T.; Emmett, M. R.; Marshall, A. G.; Sakalian, M.; Prevelige, P. E. Key Interactions in HIV-1 Maturation Identified by Hydrogen-Deuterium Exchange. *Nat. Struct. Mol. Biol.* **2004**, *11*, 676−677.

DOI: 10.1021/acs.jpcb.7b04473
J. Phys. Chem. B 2017, 121, 8263−8275

(30) Yi, Q.; Baker, D. Direct Evidence for a Two-State Protein Unfolding Transition from Hydrogen-Deuterium Exchange, Mass Spectrometry, and NMR. *Protein Sci.* **1996**, *5*, 1060−1066.
(31) Malhotra, P.; Udgaonkar, J. B. Secondary Structural Change Can Occur Diffusely and Not Modularly During Protein Folding and Unfolding Reactions. *J. Am. Chem. Soc.* **2016**, *138*, 5866−5878.
(32) Booker, G. W.; Gout, I.; Downing, K. A.; Driscoll, P. C.; Boyd, J.; Waterfield, M. D.; Campbell, I. D. Solution Structure and Ligand-Binding Site of the SH3 Domain of the P85α Subunit of Phosphatidylinositol 3-Kinase. *Cell* **1993**, *73*, 813−822.
(33) Guijarro, J. I.; Morton, C. J.; Plaxco, K. W.; Campbell, I. D.; Dobson, C. M. Folding Kinetics of the SH3 Domain of PI3 Kinase by Real-Time NMR Combined with Optical Spectroscopy. *J. Mol. Biol.* **1998**, *276*, 657−667.
(34) Jackson, S. E. How Do Small Single-Domain Proteins Fold? *Folding Des.* **1998**, *3*, R81−R91.
(35) Wani, A. H.; Udgaonkar, J. B. Revealing a Concealed Intermediate That Forms after the Rate-Limiting Step of Refolding of the SH3 Domain of PI3 Kinase. *J. Mol. Biol.* **2009**, *387*, 348−362.
(36) Dasgupta, A.; Udgaonkar, J. B. Four-State Folding of a SH3 Domain: Salt-Induced Modulation of the Stabilities of the Intermediates and Native State. *Biochemistry* **2012**, *51*, 4723−4734.
(37) Dasgupta, A.; Udgaonkar, J. B.; Das, P. Multistage Unfolding of an SH3 Domain: An Initial Urea-Filled Dry Molten Globule Precedes a Wet Molten Globule with Non-Native Structure. *J. Phys. Chem. B* **2014**, *118*, 6380−6392.
(38) Dasgupta, A.; Udgaonkar, J. B. Evidence for Initial Non-Specific Polypeptide Chain Collapse During the Refolding of the SH3 Domain of PI3 Kinase. *J. Mol. Biol.* **2010**, *403*, 430−445.
(39) Dasgupta, A.; Udgaonkar, J. B. Transient Non-Native Burial of a Trp Residue Occurs Initially During the Unfolding of a SH3 Domain. *Biochemistry* **2012**, *51*, 8226−8234.
(40) Kishore, M.; Krishnamoorthy, G.; Udgaonkar, J. B. Critical Evaluation of the Two-State Model Describing the Equilibrium Unfolding of the PI3K SH3 Domain by Time-Resolved Fluorescence Resonance Energy Transfer. *Biochemistry* **2013**, *52*, 9482−9496.
(41) Campos, L. A.; Sadqi, M.; Liu, J.; Wang, X.; English, D. S.; Muñoz, V. Gradual Disordering of the Native State on a Slow Two-State Folding Protein Monitored by Single-Molecule Fluorescence Spectroscopy and NMR. *J. Phys. Chem. B* **2013**, *117*, 13120−13131.
(42) Lakshmikanth, G.; Sridevi, K.; Krishnamoorthy, G.; Udgaonkar, J. B. Structure Is Lost Incrementally During the Unfolding of Barstar. *Nat. Struct. Biol.* **2001**, *8*, 799−804.
(43) Jha, S. K.; Udgaonkar, J. B. Direct Evidence for a Dry Molten Globule Intermediate During the Unfolding of a Small Protein. *Proc. Natl. Acad. Sci. U. S. A.* **2009**, *106*, 12289−12294.
(44) Wani, A. H.; Udgaonkar, J. B. Native State Dynamics Drive the Unfolding of the SH3 Domain of PI3 Kinase at High Denaturant Concentration. *Proc. Natl. Acad. Sci. U. S. A.* **2009**, *106*, 20711−20716.
(45) Bader, R.; Bamford, R.; Zurdo, J.; Luisi, B. F.; Dobson, C. M. Probing the Mechanism of Amyloidogenesis through a Tandem Repeat of the PI3-SH3 Domain Suggests a Generic Model for Protein Aggregation and Fibril Formation. *J. Mol. Biol.* **2006**, *356*, 189−208.
(46) Zhang, Z.; Smith, D. L. Determination of Amide Hydrogen Exchange by Mass Spectrometry: A New Tool for Protein Structure Elucidation. *Protein Sci.* **1993**, *2*, 522−531.
(47) Guttman, M.; Weis, D. D.; Engen, J. R.; Lee, K. K. Analysis of Overlapped and Noisy Hydrogen/Deuterium Exchange Mass Spectra. *J. Am. Soc. Mass Spectrom.* **2013**, *24*, 1906−1912.
(48) Weis, D. D.; Engen, J. R.; Kass, I. J. Semi-Automated Data Processing of Hydrogen Exchange Mass Spectra Using HX-Express. *J. Am. Soc. Mass Spectrom.* **2006**, *17*, 1700−1703.
(49) Arrington, C. B.; Teesch, L. M.; Robertson, A. D. Defining Protein Ensembles with Native-State Nh Exchange: Kinetics of Interconversion and Cooperative Units from Combined NMR and MS Analysis. *J. Mol. Biol.* **1999**, *285*, 1265−1275.
(50) Xiao, H.; Hoerner, J. K.; Eyles, S. J.; Dobo, A.; Voigtman, E.; Mel'čuk, A. I.; Kaltashov, I. A. Mapping Protein Energy Landscapes with Amide Hydrogen Exchange and Mass Spectrometry: I. A Generalized Model for a Two-State Protein and Comparison with Experiment. *Protein Sci.* **2005**, *14*, 543−557.
(51) Wales, T. E.; Fadgen, K. E.; Gerhardt, G. C.; Engen, J. R. High-Speed and High-Resolution UPLC Separation at Zero Degrees Celsius. *Anal. Chem.* **2008**, *80*, 6815−6820.
(52) Walters, B. T.; Ricciuti, A.; Mayne, L.; Englander, S. W. Minimizing Back Exchange in the Hydrogen Exchange-Mass Spectrometry Experiment. *J. Am. Soc. Mass Spectrom.* **2012**, *23*, 2132−2139.
(53) Bai, Y.; Milne, J. S.; Mayne, L.; Englander, S. W. Primary Structure Effects on Peptide Group Hydrogen Exchange. *Proteins: Struct., Funct., Genet.* **1993**, *17*, 75−86.
(54) Wei, G.; Xi, W.; Nussinov, R.; Ma, B. Protein Ensembles: How Does Nature Harness Thermodynamic Fluctuations for Life? The Diverse Functional Roles of Conformational Ensembles in the Cell. *Chem. Rev.* **2016**, *116*, 6516−6551.
(55) Woodward, C.; Simon, I.; Tüchsen, E. Hydrogen Exchange and the Dynamic Structure of Proteins. *Mol. Cell. Biochem.* **1982**, *48*, 135−160.
(56) Englander, S. W.; Mayne, L. Protein Folding Studied Using Hydrogen-Exchange Labeling and Two-Dimensional NMR. *Annu. Rev. Biophys. Biomol. Struct.* **1992**, *21*, 243−265.
(57) Weis, D. D.; Wales, T. E.; Engen, J. R.; Hotchko, M.; Eyck, L. F. Identification and Characterization of Ex1 Kinetics in H/D Exchange Mass Spectrometry by Peak Width Analysis. *J. Am. Soc. Mass Spectrom.* **2006**, *17*, 1498−1509.
(58) Milne, J.; Mayne, L.; Roder, H.; Wand, A.; Englander, S. Determinants of Protein Hydrogen Exchange Studied in Equine Cytochrome C. *Protein Sci.* **1998**, *7*, 739−745.
(59) Kabsch, W.; Sander, C. Dictionary of Protein Secondary Structure: Pattern Recognition of Hydrogen-Bonded and Geometrical Features. *Biopolymers* **1983**, *22*, 2577−2637.
(60) Jaswal, S. S.; Miranker, A. D. Scope and Utility of Hydrogen Exchange as a Tool for Mapping Landscapes. *Protein Sci.* **2007**, *16*, 2378−2390.
(61) Sadqi, M.; Casares, S.; Abril, M. A.; López-Mayorga, O.; Conejero-Lara, F.; Freire, E. The Native State Conformational Ensemble of the SH3 Domain from α-Spectrin. *Biochemistry* **1999**, *38*, 8899−8906.
(62) Eisenmesser, E. Z.; Millet, O.; Labeikovsky, W.; Korzhnev, D. M.; Wolf-Watz, M.; Bosco, D. A.; Skalicky, J. J.; Kay, L. E.; Kern, D. Intrinsic Dynamics of an Enzyme Underlies Catalysis. *Nature* **2005**, *438*, 117−121.
(63) Schotte, F.; Soman, J.; Olson, J. S.; Wulff, M.; Anfinrud, P. A. Picosecond Time-Resolved X-Ray Crystallography: Probing Protein Function in Real Time. *J. Struct. Biol.* **2004**, *147*, 235−246.
(64) Engen, J. R.; Smithgall, T. E.; Gmeiner, W. H.; Smith, D. L. Identification and Localization of Slow, Natural, Cooperative Unfolding in the Hematopoietic Cell Kinase SH3 Domain by Amide Hydrogen Exchange and Mass Spectrometry. *Biochemistry* **1997**, *36*, 14384−14391.

DOI: 10.1021/acs.jpcb.7b04473
J. Phys. Chem. B 2017, 121, 8263−8275